Published in final edited form as:
Nano Lett. 2011 March 9; 11(3): 1136–1140. doi:10.1021/nl104054t.

Biexciton quantum yield of single semiconductor nanocrystals from photon statistics

Gautham Nair, **Jing Zhao**, and **Moungi G Bawendi***
Department of Chemistry, Massachusetts Institute of Technology, 77 Massachusetts Avenue, Cambridge, Massachusetts 02139

Abstract

Biexciton properties strongly affect the usability of a light emitter in quantum photon sources and lasers but are difficult to measure for single fluorophores at room temperature due to luminescence intermittency and bleaching at the high excitation fluences usually required. Here, we observe the biexciton (BX) to exciton (X) to ground photoluminescence cascade of single colloidal semiconductor nanocrystals (NCs) under weak excitation in a $g^{(2)}$ photon correlation measurement and show that the normalized amplitude of the cascade feature is equal to the ratio of the BX to X fluorescence quantum yields. This imposes a limit on the attainable depth of photon antibunching and provides a robust means to study single emitter biexciton physics. In NC samples, we show that the BX quantum yield is considerably inhomogeneous, consistent with the defect sensitivity expected of the Auger nonradiative recombination mechanism. The method can be extended to study X,BX spectral and polarization correlations.

Keywords

nanocrystal; quantum dot; exciton; biexciton; antibunching; quantum yield

Many nano-structured emitters, such as colloidal semiconductor nanocrystals (NCs), can operate as single photon sources at room temperature due to the low value of the luminescence quantum yield of biexciton states (η_{bx}) compared to exciton states (η_x).[1,2] On the other hand, for a source of entangled photons and for laser applications it is best for the biexciton (BX) quantum yield to be high.[3] Emission from multiexcitonic states in NCs, our model system, is suppressed by an “Auger”-like nonradiative exciton annihilation process that is highly sensitive to particle size and composition.[4,5]

In this work we demonstrate theoretically and experimentally that η_{bx} can be conveniently obtained from the second order emission intensity correlation function, $g^{(2)}$, which is readily measured using time-correlated single photon counting systems. We show that the ratio of biexciton to exciton quantum yields is given by the normalized integrated area of the 0-time coincidence feature in the limit of weak pulsed excitation, thus providing a direct, internally-referenced measure of the BX quantum yield under mild experimental conditions.

We show that η_{bx} values from single NCs measured using our proposed method indeed agree well with independent measures of each sample’s ensemble η_{bx}. We also argue that the considerable η_{bx} inhomogeneity we observe within each sample is probably due to NC-

*To whom correspondence should be addressed mgb@mit.edu.

Additional information
The authors declare no competing financial interests. Supplementary information accompanies this paper. Correspondence and requests for materials should be addressed to M.G.B.

to-NC variation in the BX Auger decay lifetimes that has been previously obscured by ensemble averaging. Due to rapid emission intermittency ("blinking") and the limited photostability of single NCs under high excitation fluence, it would have been prohibitively difficult to accurately measure these η_{bx} values using conventional methods that require population modeling across an experimental high power excitation fluence series. Moreover, our method does not make use of spectral or temporal resolution of the BX and X emission.

We observed individual colloidal CdSe/CdZnS (core/shell) nanocrystals by confocal sample-scanned microscopy using an oil immersion microscope objective and a 414 nm pulsed diode laser for excitation (2.5MHz, ≈ 30 ps pulsewidth). The collected emission was split and detected by two APD-based single photon detector modules in a Hanbury-Brown-Twiss geometry. The intensity time traces of each channel and the $g^{(2)}$ histogram were simultaneously recorded. For further details, see Methods section.

The second order cross correlation function $g^{(2)}(\tau)$ is defined as:

$$g^{(2)}(\tau)=\frac{\langle I_1(t)I_2(t+\tau)\rangle}{\langle I_1(t)\rangle\langle I_2(t+\tau)\rangle} \quad (1)$$

where $I_1(t)$ and $I_2(t)$ are the signal intensities of the two channels and the brackets denote expectation values. For an emitter under pulsed excitation the $g^{(2)}$ curve consists of a series of discrete peaks as shown schematically in Figure 1a. The amplitude of the center (0-time) peak reflects the probability that two photons were detected within a single laser cycle while any of the two adjacent $\tau \approx \pm t_{rep}$ peaks originate when two photons are detected one each in consecutive laser cycles. The ratio of the integrated area of the center and side features, hereafter referred to as $g_0^{(2)}$, is given by:[6]

$$g_0^{(2)} \equiv \frac{\int_{-\Delta t}^{\Delta t} g^{(2)}(\tau)d\tau}{\int_{t_{rep}-\Delta t}^{t_{rep}+\Delta t} g^{(2)}(\tau)d\tau}=\frac{\langle n(n-1)\rangle}{\langle n\rangle^2}, \quad (2)$$

where the random variable n is the total number of photons emitted after an individual excitation pulse and Δt is an appropriate integration range. A detailed derivation is given in the Supplementary information.

The emission of a single NC under pulsed excitation is governed by two types of random processes. Firstly, the NC absorbs a Poisson-distributed random number of photons N. The resulting N electrons and holes recombine one by one in a cascade to the ground state, each step of which can be radiative or nonradiative ($\xi_m = 1$ or $\xi_m = 0$, respectively). In the limit that $\langle N\rangle \to 0$ it can be shown that (see Supplementary):

$$g_{0\,\mathrm{NC}}^{(2)}=\frac{\langle n_{\mathrm{NC}}(n_{\mathrm{NC}}-1)\rangle}{\langle n_{\mathrm{NC}}\rangle^2} \to \frac{\langle \xi_1\xi_2\rangle}{\langle \xi_1\rangle^2} \approx \frac{\eta_{bx}}{\eta_x} \quad (3)$$

Here $\eta_x = \langle\xi_1\rangle$ and $\eta_{bx} = \langle\xi_2\rangle$ are the luminescence quantum yields of the 1e-1h ("exciton" or X) and 2e-2h ("biexciton" or BX) configurations respectively, and it has been assumed that the X and BX fluorescence processes are independent of each other (see Supplementary Information). Therefore, at very low powers when $\langle N\rangle \to 0$ a residual 0-time peak will persist in the normalized $g^{(2)}(\tau)$ due to biexciton emission. The size of the center 0-time peak reflects the likelihood of biexciton creation and subsequent two-photon emission. The probability of this event vanishes as $\langle N\rangle^2$. The side peaks are due to creation and emission of two excitons in consecutive laser cycles. The probability of creation and emission of two

excitons in consecutive laser cycles, which involves absorption from two consecutive pulses, also vanishes as $\langle N\rangle^2$. Therefore, $g^{(2)}_{0\ \mathrm{NC}}$ approaches a constant value, η_{bx}/η_x, as $\langle N\rangle \rightarrow 0$ even though biexcitons are created only very rarely when compared to excitons. The calculated curves shown in Figure 1b illustrate that, unlike the fraction I_{mx}/I_{tot} of total emission due to multiexcitons, $g^{(2)}_0$ does not go to zero at low powers. For NCs under weak continuous excitation, instead of pulsed excitation, an analogous argument to the above (detailed in the Supplementary) gives $g^{(2)}(\tau=0)/g^{(2)}(\tau\rightarrow\infty)=\eta_{bx}/\eta_x$.

Figure 2 shows data from an experiment on a single CdSe/CdZnS NC under pulsed weak excitation. We ensured that our data is representative of the $\langle N\rangle \rightarrow 0$ limit by operating far below signal saturation, in a regime where the measured $g^{(2)}_0$ was insensitive to ±50% changes in the excitation power. In all of the NCs that we studied, the center peak clearly rises above the noise levels. More importantly, the sizes of the center peak in our $g^{(2)}$ are well above those attributable to extraneous sources such as stray light or neighboring NCs (see Methods). Therefore we assign the 0-time coincidence feature to cascaded BX,X emission. The data shown in Figure 2 implies a BX to X quantum yield ratio of $\eta_{bx}/\eta_x=g^{(2)}_0\approx 0.06$.

For our digitally blinking NCs, the measured $g^{(2)}_0$ is a direct estimate of the biexciton emission quantum yield because, as we show below, the relevant value of the X QY is nearly unity ($\eta_x\approx 1$). Our photon cross-correlation histograms are accumulated over a period of time during which η_x and potentially η_{bx} can change stochastically due to blinking.[7] Because the 0-time and the side peak are collected in parallel and then divided to obtain $g^{(2)}_{0\ \mathrm{NC}}$ it can be shown that:

$$g^{(2)}_{0\ \mathrm{NC}}=\frac{\langle \eta_x(t)\eta_{bx}(t)\rangle_t}{\left\langle \eta_x(t)^2\right\rangle_t} \tag{4}$$

Where $\langle\cdot\rangle_t$ denotes a time average over the course of each experiment (details in Supplementary Information). It is seen that $g^{(2)}_0$ weighs more heavily the η_x and η_{bx} values during bright periods. For the case of binary on-off digital blinking exhibited by the majority of NCs studied, $g^{(2)}_{0\ \mathrm{NC}}$ reduces to $\eta^{\mathrm{on}}_{bx}/\eta^{\mathrm{on}}_x$. This result is not altered by rapid on-off switching even down to μs timescales since we focus only on the $|\tau|\lesssim t_{rep}<1$ μs region of $g^{(2)}(\tau)$. Furthermore, Brokmann et al.[8] and Fisher et al.[9] have found that the X quantumefficiency for digitally blinking NCs during on-periods (η^{on}_x) can be well approximated by unity. Therefore $g^{(2)}_0\approx\eta^{\mathrm{on}}_{bx}$ for our single NC measurements.

Figure 3 shows a summary of our data on a total of 44 individual NCs from five different samples with varying size and composition, and serves as a test of our conclusion that $g^{(2)}_0\approx\eta^{\mathrm{on}}_{bx}$ for digitally-blinking NCs. The samples are CdSe/CdZnS NCs with emission at 627 nm, 642 nm, 648 nm, and 655 nm prepared by high temperature pyrolysis,[10] and commercial QDOT655 with emission at 655 nm. First, the $g^{(2)}_0$ values we measure are seen to correlate well with the BX lifetimes (τ_{bx}) we independently estimated by fitting ensemble transient PL data from each sample[11] (See Methods, Supplementary). This is as expected since $\eta_{bx}=k^{rad}_{bx}\tau_{bx}$, where the BX radiative rate (k^{rad}_{bx}) was found to be similar for many CdSe-based samples.[11] Second, the average $g^{(2)}_0\approx 0.15$ for NCs in the QDOT655 sample is found to be in good agreement with the ensemble $\eta_{bx}\approx 0.11$ previously reported by Fisher et al.[12]

for the same sample and the $\eta_{bx} \approx 0.12$ we estimate from our tPL data (see Supplementary), confirming the connection between $g_0^{(2)}$ and the BX emission efficiency.

We observe significant spreads, shown in Figure 3, of the η_{bx} values obtained by averaging repeated measurements on different individual NCs within each sample. This NC-to-NC inhomogeneity is ≈ ±0.013 for the sample with emission at 627 nm and greater than ±0.04 for the two samples with emission at 655 nm, whereas repeated measurements of $g_0^{(2)}$ on the same single NC varies only by ≈ ± 0.005 or, for a QDOT655 NC by ≈ ± 0.015. The smaller variance for repeated measurements on the same NC indicates significant NC-to-NC inhomogeneity in the BX quantum yield, which in turn can be attributed to changes in k_{bx}^{rad}, τ_{bx}, or both. Since both band edge 1S electron states are occupied in a BX, there are no dark configurations and k_{bx}^{rad} is determined primarily by the spatial overlap of the electron and hole wavefunctions (see discussion in Supplementary Information). Large changes in this overlap are not expected.

An inhomogeneous τ_{bx} within a sample is plausible because the Auger relaxation process is strongly dependent on electronic defects. Spatially smooth wavefunctions have little overlap with the high kinetic energy final state resulting from Auger relaxation, so it is believed that the process is efficient in NCs because of lattice defects that "roughen" the ground particle-in-a-box states.[5] Subtle variations in the quality and smoothness of the core/shell and shell/ligand interfaces could therefore affect the sensitive Auger mechanism without affecting other observables like η_x, radiative rates, or emission wavelengths in measurable or systematic ways. The inhomogeneity in τ_{bx} evidenced in our data can be easily hidden in ensemble studies since it affects only the long tail of the averaged BX decay, which is difficult to isolate from the overlapped X dynamics (see discussion in Supplementary). In comparison, the η_{bx} variation is clearly evident in the single NC measurements demonstrated in this work.

The quantitative connection explored here between $g^{(2)}$ and the biexciton quantum yield has important implications for the routine use of $g^{(2)}$ data in PL microscopy. A $g^{(2)}(\tau)$ measurement essentially reports on the probability distribution of the time-separation (τ) between pairs of photons emitted by a source. When $g^{(2)}(\tau)$ shows a dip at $\tau = 0$, the source is said to be "antibunched", considered the signature of a quantum emitter.[1] In fact, even under weak excitation, strong anti-bunching from a single emitter requires an efficient mechanism to suppress multiphoton emission or block its detection,[1] such as the impossibility of two-photon absorption in atoms,[13] spectral separation of exciton and multiexciton lines in epitaxial quantum dots,[14] or BX emission quenching by the Auger mechanism in NCs. Therefore, strong antibunching is a sufficient condition for establishing that a single emitter has been isolated, but it is commonly and incorrectly assumed that it is also a necessary condition. If the possibility of a 0-time low-power residual feature due to BX emission is not contemplated, fluorophores that show appreciable signal at $\tau = 0$ will be judged as not being properly isolated single emitters. Such selection bias against emitters with appreciable η_{bx} affected our earlier work on the photon statistics of single CdSe-based NCs.[12] In that work, a small $\tau = 0$ feature was used as a pre-condition for further measurements, effectively selecting only NCs that we now know had η_{bx} well below the sample average.

We illustrate the mechanistic insights that are facilitated by the direct relationship discussed here between $g_0^{(2)}$ and η_{bx} by applying it to recent published data on NCs that reportedly display suppressed blinking. Mahler et al.[15] and then Spinicelli[16] et al. in a follow-up reported CdSe/CdS (core/shell) NCs that switch between an on state and a "grey" state with

appreciable fluorescence. More recently, Wang et al.[17] have reported ZnCdSe/ZnSe (core/shell) NCs that emit steadily without observable blinking. Both groups report strong antibunching with $g^{(2)}(0) \approx 0$, which we have shown here implies that a highly efficient pathway for annihilation of the BX remains. However, the authors attribute blinking suppression to suppression of the Auger mechanism itself, because the traditional charging model of blinking[18] proposes that off-state PL quenching is also caused by an Auger transfer to an uncompensated electron or hole in the NC volume. Our results show that the proposed interpretation and mechanism is compatible with their observation that $g^{(2)}(0) \approx 0$ only if it can be shown that the Auger decay rates for charged excitons and biexcitons are very different (For example, it is possible that the Auger decay rates for negative and positive trions are very different.) or that an alternative efficient BX decay mechanism exists.

In summary, we have shown theoretically that η_{bx}/η_x is given by the size of the 0-time feature in an emitter's $g^{(2)}$ function. Experimentally, we have shown that the technique correctly measures the average η_{bx} of NC samples and also reveals NC to NC inhomogeneity in BX physics. Strong antibunching (i.e. $g_0^{(2)} \approx 0$) requires both isolation of a single emitter and efficient suppression or spectral filtering of multiexciton emission.

Methods

Experiment

Colloidal CdSe/CdZnS (core/shell) nanocrystals were prepared using standard methods.[10] One of the samples were commercial QDOT655 NCs from Quantum Dot Corporation. Samples were spun cast from a toluene/poly-(methylmethacryllate) solution onto glass coverslips. Individual nanocrystals were observed by confocal sample-scanned microscopy using an oil immersion microscope objective (100x, 1.40 NA, Plan Apochromat) for excitation from a pulsed diode laser (414 nm, 2.5MHz, ≈ 30 ps pulsewidth). Typical excitation fluences were 12 μJ/cm^2 (30 nW average power). Some of the signal was dispersed onto a CCD camera for spectral recording. The rest was split and focused onto APD-based single photon detector modules (Perkin Elmer) in a Hanbury-Brown-Twiss geometry using suitable spectral filters. Intensity time traces and $g^{(2)}$ were simultaneously recorded using pulse counters and a correlator card (Timeharp 200). Ensemble transient PL of samples dispersed in hexane were taken using a streak camera (Hamamatsu C5680) with 400nm excitation derived from a 1kHz amplified Ti:sapphire laser. All measurements were done under ambient conditions.

Analysis

In a real experiment there are extraneous sources of light other than BX emission that may contribute to $g_0^{(2)}$. First a temporally uniform background from detector dark counts was subtracted from $g^{(2)}$ histograms before calculating $g_0^{(2)}$. Second, to account for a pulsed background, like laser scatter, we assumed b_j are the fraction of the average start and stop channel intensities due to the pulsed background and calculated $g_0^{(2)}$, which gives $g_0^{(2)} = 1 - (1 - b_1)(1 - b_2)(1 - g_{0\,\mathrm{NC}}^{(2)}) \approx g_{0\,\mathrm{NC}}^{(2)} + b_1 + b_2$. Lastly, if there is another identical NC somewhere within the collection volume, and it is responsible for a fraction $y_i = 1 - x_i$ of the signals in channels $j = 1,2$, then $g_0^{(2)} = g_{0\,\mathrm{NC}}^{(2)} + (x_1 y_2 + x_2 y_1)(1 - g_{0\,\mathrm{NC}}^{(2)})$. Derivations of these identities are given in the Supplementary Information. The quantities $b_{1,2}$ and $y_{1,2}$ can be estimated from a clear area in the sample, from which we find that extraneous sources can account for a $g_0^{(2)} \approx 0.003$. A significantly more conservative upper bound of $g_0^{(2)} \approx 0.015$ can be obtained based on the darkest off-state intensities observed during PL time traces. Since

this off-state signal is likely due to weak emission from the NC itself, we consider the $g_0^{(2)} \approx 0.003$ estimate more appropriate.

Supplementary Material

Refer to Web version on PubMed Central for supplementary material.

Acknowledgments

This work was supported in part by the Department of Energy (Grant No. DE-FG02-07ER46454) and the Harrison Spectroscopy Laboratory (Grant No. NIH P41 RR02594). G.N. was funded during the concluding portion of this work as part of the Center for Excitonics, an Energy Frontier Research Center funded by the U.S. Department of Energy, Office of Science, Office of Basic Energy Sciences under Award Number DE-SC0001088. The authors would like to thank Yinthai Chan, Hee-Sun Han, and Cliff R. Wong for help in sample preparation and Cassandra Cox for experimental assistance.

References

1. Lounis B, Orrit M. Rep. Prog. Phys. 2005; 68:1129.
2. Yuan Z, Kardynal BE, Stevenson RM, Shields AJ, Lobo CJ, Cooper K, Beattie NS, Ritchie DA, Pepper M. Science. 2002; 295:102. [PubMed: 11743163]
3. Stevenson RM, Young RJ, Atkinson P, Cooper K, Ritchie DA, Shields AJ. Nature. 2006; 439:179. [PubMed: 16407947]
4. Robel I, Gresback R, Kortshagen U, Schaller RD, Klimov VI. Phys. Rev. Lett. 2009; 102:177404. [PubMed: 19518831]
5. Efros, AL.; Lockwood, DJ.; Tsybeskov, L. Semiconductor nanocrystals, from basic principles to applications. Kluwer Academic; 2003.
6. Santori C, Fattal D, Vuckovic J, Solomon GS, Yamamoto Y. New J. Phys. 2004; 6:1.
7. Nirmal M, Dabbousi BO, Bawendi MG, Macklin JJ, Trautman JK, Harris TD, Brus LE. Nature. 1996; 383:802.
8. Brokmann X, Coolen L, Dahan M, Hermier J-P. Phys. Rev. Lett. 2004; 93:107403. [PubMed: 15447451]
9. Fisher BR, Eisler HJ, Stott NE, Bawendi MG. J. Phys. Chem. B. 2004; 108:143.
10. Snee P, Chan Y, Nocera DG, Bawendi MG. Adv. Mater. 2005; 17:1131.
11. Nair G, Bawendi MG. Phys. Rev. B. 2007; 76:081304(R).
12. Fisher BR, Caruge J-M, Zehnder D, Bawendi MG. Phys. Rev. Lett. 2005; 94:087403. [PubMed: 15783930]
13. Kimble HJ, Dagenais M, Mandel L. Phys. Rev. Lett. 1977; 39:691.
14. Thompson RM, Stevenson RM, Shields AJ, Farrer I, Lobo CJ, Ritchie DA, Leadbeater ML, Pepper M. Phys. Rev. B. 2001; 64:201302(R).
15. Mahler B, Spinicelli P, Buil S, Quelin X, Hermier J-P, Dubertret B. Nat. Mater. 2008; 7:659. [PubMed: 18568030]
16. Spinicelli P, Buil S, Quélin X, Mahler B, Dubertret B, Hermier J-P. Phys. Rev. Lett. 2009; 102:136801. [PubMed: 19392384]
17. Wang X, Ren X, Kahen K, Hahn MA, Rajeswaran M, Maccagnano-Zacher S, Silcox J, Cragg GE, Efros AL, Krauss TD. Nature. 2009; 459:686. [PubMed: 19430463]
18. Efros AL, Rosen M. Phys. Rev. Lett. 1997; 78:1110.

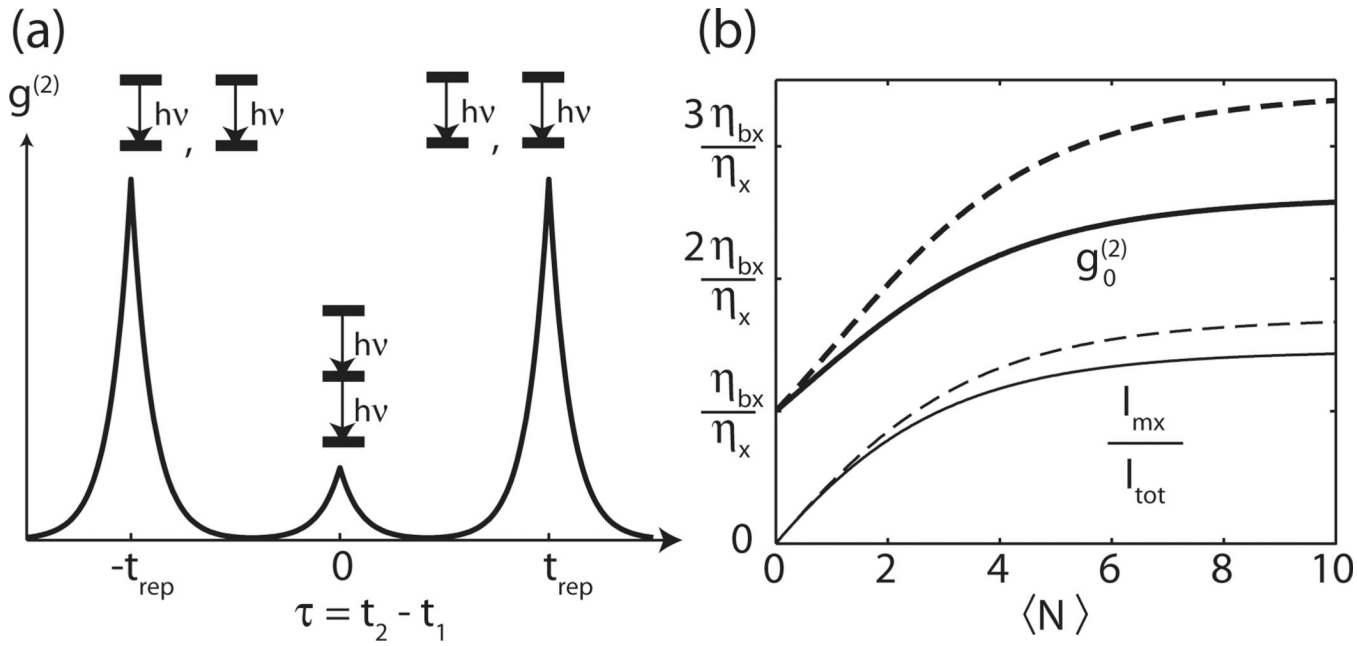

Figure 1.

(a) Schematic illustrating the main features of $g^{(2)}$ (τ) on a single colloidal nanocrystal under pulsed excitation with repetition rate t_{rep}^{-1}. The shape of the center and the side peaks is the same because the distribution of the time differences between BX,X photons and the time differences between consecutive X,X photons are both defined only by the X lifetime. (b) Calculation of the excitation power dependence of $g_0^{(2)}$, the ratio of the center to $+t_{rep}$ integrated peak areas, and I_{mx}/I_{tot}, the fraction of the total emission intensity due to multiexcitons, for a CdSe-like NC. The calculated result is plotted in units of η_{bx}/η_x, the ratio of the biexciton to exciton fluorescence quantum yields. $\langle N \rangle$ is the average number of photons absorbed. Solid curves are for the case where $\eta_{bx}/\eta_x = 0.1$ and the dashed curve represents the case where $\eta_{bx}/\eta_x \rightarrow 0$. A simple Auger decay scaling model described in detail in the Supplementary information was used to approximate values for the quantum yields of higher multiexcitons based on the assumed η_{bx}. For small $\langle N \rangle$, $g_0^{(2)}$ grows linearly from its η_{bx}/η_x intercept and then saturates at high powers owing to the diminishing quantum yield of higher multiexcitons.

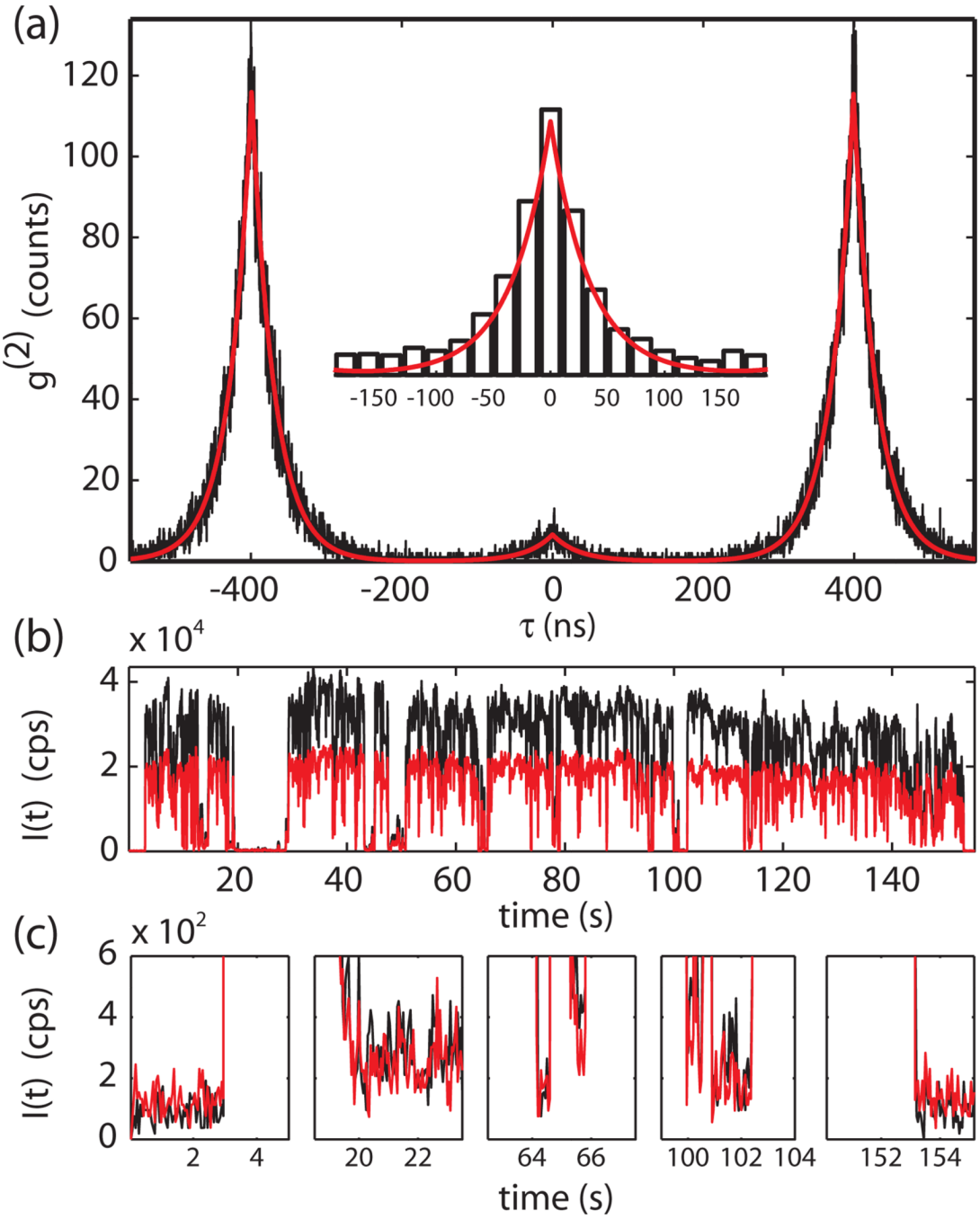

Figure 2.

(a) Measured, unnormalized $g^{(2)}$ (τ) from a single CdSe/CdZnS NC under ≈ 12 μJ/cm^2 pulsed excitation, representative of the $\langle N \rangle \ll 1$ limit. The normalized integrated area of the center feature, $g_0^{(2)} = 0.06$, is a direct measure of the BX to X quantum yield ratio of this NC. Inset is a 20ns-binned detail of the center peak. Red lines are a fit to the sum of three two-sided exponentials. (b) Time traces of intensity in start and stop channels (black and red) during the $g^{(2)}$ acquisition. (c) Details showing off-state intensities. The events in the first and last panel correspond to switching the excitation laser on and off.

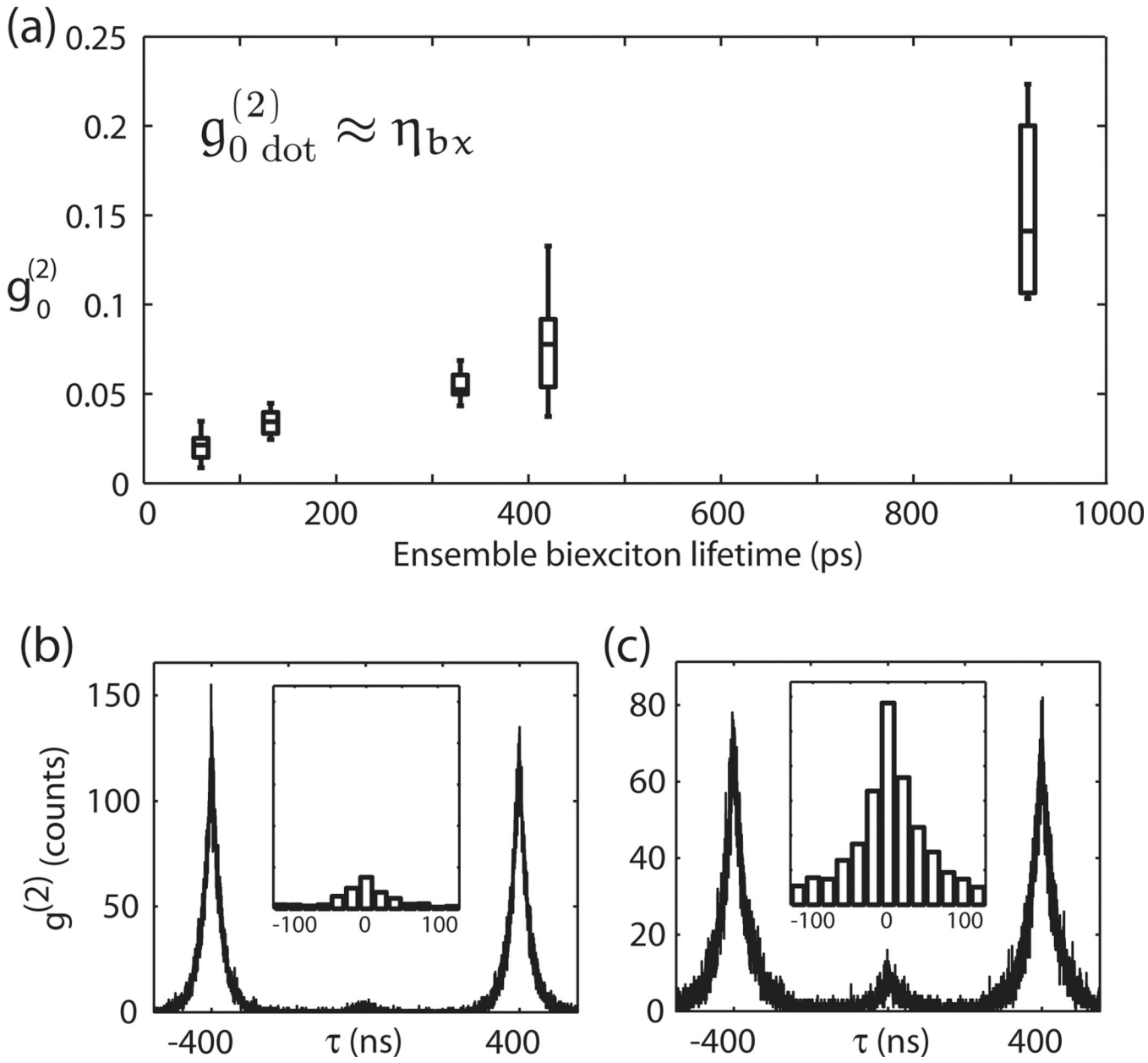

Figure 3.

(a) Box and whiskers plot of our measured values of $g_0^{(2)}$ on several individual NCs from five different samples plotted against each sample's ensemble biexciton lifetime. The box edges indicate the first and third quartiles, the line within indicates the median value, and the external lines the minimum and maximum. For a colloidal, digitally blinking, CdSe-based NC, $\eta_x^{\mathrm{on}} \approx 1$ so $g_0^{(2)} \approx \eta_{bx}$. (b) Raw $g^{(2)}$ data of an NC from the sample with the shortest BX lifetime. In this case $g_0^{(2)} = 0.021\%$. Inset shows a 20ns-binned detail of the center feature. (c) Same as (b) but for an NC from the sample with the longest BX lifetime, showing $g_0^{(2)} = 0.128$.